Technoeconomic Analysis of Infrastructure for Transporting Captured CO_2 to Central Conditioning Unit

Pedersen, Rikke Cilius; Elmegaard, Brian; Jensen, Jonas K.

Published in:
Proceedings of the 17th International Conference on Greenhouse Gas Control Technologies

Publication date:
2025

Document Version
Publisher's PDF, also known as Version of record

17th International Conference on Greenhouse Gas Control Technologies, GHGT-17

20th -24th October 2024 Calgary, Canada

Technoeconomic analysis of infrastructure for transporting captured CO_2 to central conditioning unit

Rikke C. Pedersen [a]*, Brian Elmegaard [a], and Jonas K. Jensen [a]

[a] *Technical University of Denmark, Dept. of Civil & Mechanical Eng., Kgs. Lyngby, DK*

Abstract

Carbon capture from bio-methane production will be an important tool in the Danish climate strategy towards 2050. These point sources are relatively small, remotely located, and can likely benefit from shared transport infrastructures. In this paper, a system comprising the compression and transport of impure CO_2 in a gaseous state through a pipeline from a small production site to a central conditioning unit was analyzed. A technical model was made, which served as the basis for an economic analysis. The gas was delivered at two different pressure levels to the shared central conditioning unit. The effects of varying gas flow rates and transport distances were investigated and the economic optimal pipeline diameter for each case was identified. Furthermore, a sensitivity analysis of relevant economic assumptions was performed to determine whether the investigated parameters affected the optimal diameter and costs. It was found, that the delivery of gas at 2 bar at the central unit compared to 18 bar was cheaper, except for the longest investigated distances and smallest mass flow rates. The importance of choosing the optimal pipe size became more important as the transport distance increased and as the mass flow rate decreased. The estimated capital investment of the pipeline showed to be the most sensitive parameter while the compressor efficiency was the least important parameter. The results of the study can be used in future analyses to benchmark the costs of local conditioning at small point sources to that of a shared central conditioning system.

Keywords: CO_2 pipeline transport; CO_2 compression; CCUS infrastructure, Technoeconomic analysis

1. Introduction

Part of the Danish climate strategy is to replace all natural gas with bio-methane produced from livestock manure. CO_2 from biogas facilities is expected to account for 12 % of the total carbon capture potential in Denmark in 2040 and is distributed on more than 50 minor point sources [1]. The production facilities are typically located in open farmland to minimize the transport costs of the biomass. Today, CO_2 capture through amine absorption or membrane technologies is implemented in 80 % of the Danish biogas production facilities [2], as the CO_2 must be removed from the biogas before the gas is sent to the national gas grid. The CO_2 is biogenic and holds the potential to achieve negative emissions through permanent storage or can be used for the production of green fuels through utilization. However, before the CO_2 can be sent to an off-taker it must be conditioned to the correct purity and state according to specifications set out by the off-taker.

It might not be economically feasible to perform the conditioning of the CO_2 on-site, as the biogas facilities are relatively small emitters. It is estimated that the emission size of existing biogas facilities in Denmark ranges between 1000 t CO_2 to 60 000 t CO_2 per year [1]. Co-utilization of infrastructure is expected to yield economic benefits for the emitters and be more efficient than single-source to single-sink transportation when carbon capture, utilization, and storage is to be implemented on a large scale within a limited geographical area [3]. This will especially be important for smaller emitters [4]. However, it is still unsure how remotely located small emitters such as biogas facilities are best included in a common infrastructure. There are two relevant options for transporting the CO_2 onshore from such plants, either through trucks or pipelines. The current standards for truck transport require the CO_2 to be in a liquid state, while pipelines are more flexible as transport in the gaseous state is possible.

Transport of CO_2 in short distances through pipelines has been analyzed in several studies. Knoope *et al.* [5] perform

* Corresponding author. Email address: rikpe@dtu.dk

economic optimizations of CO_2 pipeline configurations and find that gaseous state is more cost-effective for small mass flow rates and short distances. They also find that the requirements for materials are lower when considering transport in a gaseous state. The same conclusions are achieved by Lu *et al.* [6]. For transport of unconditioned CO_2 through pipelines, impurities must be considered as these affect the properties of the fluid. Vitali *et al.* [7] emphasize that even though transport of CO_2 through pipelines is a well-known technology, transport of CO_2 with impurities require further research. Kolster *et al.* [3] find that a greater content of incondensable gases generally increases the pipeline diameter. However, for transport distances below 30 km, there is no change in pipeline costs with purity.

When making an economic evaluation of the transport infrastructure for CO_2 it is emphasized by Roussanaly *et al.* [4] that a detailed cost model taking the flow rate, transport mode, and transport distance into account is required. Onyebuchi *et al.* [8] find that a detailed technical model including material and fluid properties must be considered to determine the economic optimal pipe diameter for pipeline transport of CO_2. Skaugen *et al.* [9] make a detailed technical and economic model of pipelines for transport of CO_2 with impurities. They find that the presence of impurities increases the transportation costs by 20 % to 40 % compared to pure CO_2.

In this paper, we investigate a subsystem of an infrastructure shared amongst several biogas facilities. A technoeconomic analysis is made to evaluate how various flow rates of CO_2 and transport distances affect the costs of transporting unconditioned gaseous CO_2 from a small biogas facility through a pipeline to a central conditioning system located at a nearby plant. The paper aims to map the costs under two different assumptions, first that the CO_2-mix must be delivered at high pressure so that the central conditioning unit only entails purification and liquefaction, and second it is delivered at low pressure meaning that the compression is also performed centrally. The optimal pipe sizes for the investigated cases are presented and a sensitivity analysis is made on chosen parameters to determine their influence on costs.

Nomenclature

Roman Letters

$\dot{m}$	Mass flow rate [kg s^{-1}]
$\dot{Q}$	Heat transfer rate [W]
$\dot{V}$	Volume flow rate [m^3 s^{-1}]
$\dot{W}$	Power [W]
A	Area [m^2]
D	Diameter [m]
d	Burial depth [m]
f	Friction factor [–]
H	Height [m]
h	Specific enthalpy [J kg^{-1}]
k	Souders-Brown constant [m s^{-1}]
L	Length [m]
m_{spec}	Specific mass [kg m^{-1}]
p	Pressure [bar]
R	Thermal resistance [K W^{-1}]
r	Discount rate [%]
S_f	Shape factor [–]
T	Temperature [°C]
t	Wall thickness [m]
U	Overall heat transfer coefficient [W (m^{2}K)$^{-1}$]
u	Velocity [m s^{-1}]
X	Size factor
Y	Lifetime [years]
Re	Reynolds number [–]

Greek Letters

α	Scaling factor
λ	Thermal conductivity [W (mK)$^{-1}$]
ρ	Density [kg m^{-3}]
σ	Material strength [bar]
ε	Surface roughness [m]

Subscripts and Superscripts

j	Component
abs	Absolute
amb	Ambient
CA	Corrosion allowance
comp	Compression
cool	Process cooling
el	Electricity
fix	Fixed
i	Inner
in	Inlet
lm	Logarithmic mean
o	Outer
rel	Relative
t	Tensile
y	Yield

Abbreviations

CAPEX	Capital expenses [EUR]
DN	Nominal diameter [mm]
LC	Levelized costs [EUR kg^{-1}]
NPS	Nominal pipe size
OPEX	Opeartional expenses [EUR y^{-1}]
PEC	Purchased equipment cost [EUR]
ROW	Right-of-Way

2. Methods

2.1. Case description

The system investigated in this paper consists of a compression process followed by transport of the CO_2 mixture in a gaseous state through a pipeline (Fig 1). During compression, intercooling was used to cool the gas and simultaneously remove water condensate. The composition and state of the CO_2 feed gas at the inlet of the compression process are given in Table 1.

Table 1. Composition and state of the captured CO_2 feed gas entering the compressor train.

CO_2	H_2O	N_2	O_2	Pressure	Temperature
97 %-dry	saturated	2 %-dry	1 %-dry	1.5 bar	40 °C

The compression of the feed gas should be great enough to overcome the pressure loss in the pipeline and ensure that the gas is delivered at the correct pressure level at the outlet of the pipeline. Two cases were considered for the delivery pressure (Fig 1). In option 1, the CO_2 mixture should be delivered at 2 bar to enter the compressor train of the conditioning system at the nearby plant. In option 2, the CO_2 mixture was assumed to enter only the liquefaction and purification process at the nearby plant, meaning that the gas should be delivered at 18 bar. To map the effects of different plant sizes and transport distances, the following variables were investigated: The mass flow rate of the captured feed gas and the length of the pipeline. The variables were varied between 0.5 th^{-1} to 10 th^{-1} and 1 km to 35 km, respectively.

2.2. Mixture model

The CO_2 mixture contained impurities. The Peng-Robinson equation of state [10] has shown good prediction of thermodynamic properties for CO_2 mixtures at reasonable computational effort [6]. Therefore, the Enhanced Predictive Peng-Robinson equation of state proposed by Jaubert and Mutelet [11] was used to model the mixture. It uses temperature dependent binary interaction parameters which are determined using a group contribution method. The group contribution constants presented by Xu *et al.* [12] were used. The viscosity of the mixture was determined using a corresponding states model for fluids containing large amounts of CO_2 proposed by Chapoy *et al.* [13], which has shown good prediction performance [7]. The mixture model was implemented in the software Engineering Equation Solver (EES) [14].

2.3. Compression model

The feed gas was compressed through a compressor train with intercooling. During intercooling part of the water content condensed and was removed in subsequent gas-liquid separators before the next compressor. Therefore, the mass flow rate at the pipeline inlet was slightly lower than the entering feed gas. The number of compressors was chosen for each specific case to ensure that the pressure ratio did not exceed four and equal pressure ratios were applied to all compressors. For feed gas flow rates of less than 500 m^3h^{-1} reciprocating compressors were used with isentropic efficiencies of 70 % and for greater flow rates screw compressors were used with an isentropic efficiency of 75 % [15]. The compressor sizes were evaluated based on the required power consumption, $\dot{W}$, as outlined in Table 2.

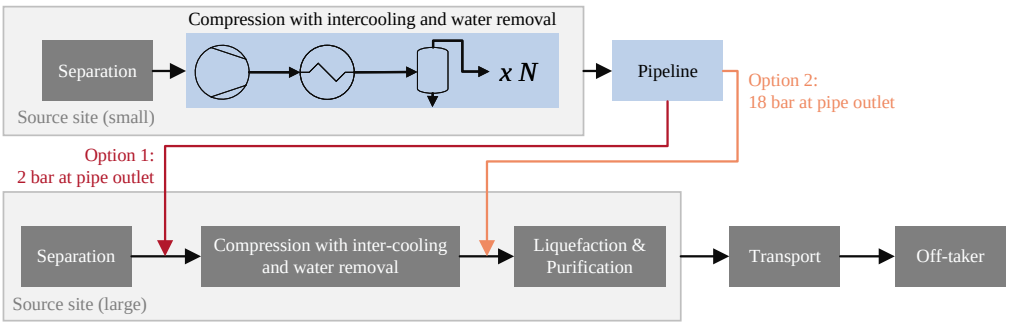

Fig 1. Flowchart of overall system. The processes in light blue are the focus of this study. The two options for delivery pressures are shown with the red and orange arrows.

The intercoolers were plate heat exchangers with a minimum temperature difference of 10 K. An overall heat transfer coefficient, U, of 300 W (m^2K)$^{-1}$ was used with the logarithmic mean temperature difference, ΔT_{lm}, to estimate the required heat transfer area, A_{heat}, as given in Table 2. For heat exchangers with phase change, this approach would lead to slightly wrong estimations. However, the error was expected to be insignificant for the overall economic results. It was assumed that cooling water was heated from 30 °C to 45 °C. Therefore, the gas was 40 °C at the inlet of each compressor and the pipeline. Gas-liquid separators were modeled as vertical vessels using the Souders-Brown equation [16] assuming a k-value of 0.11 m s^{-1} [17] and the size relation given in Table 2. Pressure and heat losses were neglected in the compression process.

Table 2. Size factors and relations for each component type.

Component Type	**Sizing Factor, X_j**	**Sizing Relation**
Compressors	Power ($\dot{W}$)	$\dot{W} = \dot{m}\Delta h$
Heat exchangers	Heat transfer area (A_{heat})	$A_{\mathrm{heat}} = \dot{Q}/(U\Delta T_{\mathrm{lm}})$
Gas-liquid separators	Product of height and diameter ($HD^{3/2}$)	$u = k\sqrt{(\rho_{\mathrm{liq}} - \rho_{\mathrm{gas}})/\rho_{\mathrm{gas}}}$, $A_{\mathrm{cross}} = \dot{V}_{\mathrm{gas}}/u$, $D = \sqrt{4A_{\mathrm{cross}}/\pi}$, $H/D = 3$

2.4. Pipeline model

The dimensions of the pipeline were chosen between available Nominal Pipe Sizes (NPS) [18] which relates the nominal diameter (DN) to a thickness. The wall thickness, t, should be great enough for the pipe to withstand the maximum pressure occurring at the inlet of the pipe. It was given from Barlow's formula shown in Equation (1), where a corrosion allowance (CA) of 3.15 mm was included [17]. The required thickness was increased by 12.5 % to allow for manufacturing defects [9].

$$t = 1.125 \cdot \left(\frac{p_{\max} D_i}{2\sigma_{\max}} + t_{\mathrm{CA}} \right) \tag{1}$$

The maximum allowed stress, σ, was chosen based on the guidelines in the European Pressure Directive (PED) [19] and is given in Equation (2). The pipeline was assumed to be of 316 stainless steel to reduce corrosion from the presence of H_2O and O_2 in the gas. Yield, σ_{y}, and tensile, σ_{t}, strengths of 170 MPa and 485 MPa, respectively, were used [20].

$$\sigma_{\max} = \mathrm{Min}\left(\frac{2}{3}\sigma_{\mathrm{y}}, \frac{5}{12}\sigma_{\mathrm{t}} \right) \tag{2}$$

Several pipe diameters were investigated for each combination of mass flow rate and distance to find the one resulting in the overall lowest costs. A smaller pipe diameter will increase the velocity and hence pressure drop, which increases the costs associated with the compression process. A larger diameter is typically more expensive to install and thereby increases the capital expenses of the pipeline.

The pipeline was modeled considering pressure loss and heat transfer with the ambient assuming a homogenous flow. It was divided into segments to discretize the losses over the whole length of the pipeline. The pressure and temperature at the outlet of the previous segment were used to evaluate the properties at the inlet of the next segment. The pressure loss associated with friction was determined for incompressible flow using the friction factor, f, suggested by the White-Colebrook law given in Equation (3) [21]. The relative roughness, $\varepsilon_{\mathrm{rel}}$, was given from an absolute roughness of 0.002 [21] and the internal pipe diameter. The pressure loss associated with friction, Δp, was given by Equation (4).

$$\frac{1}{\sqrt{f}} = -2\log\left(\frac{\varepsilon_{\mathrm{rel}}}{3.71} + \frac{2.51}{\mathrm{Re}\sqrt{f}} \right) \quad \text{with} \quad \varepsilon_{\mathrm{rel}} = \frac{\varepsilon_{\mathrm{abs}}}{D_{\mathrm{i}}} \tag{3}$$

$$\Delta p = \frac{1}{2}\rho u^2 f \frac{L}{D_{\mathrm{i}}} \tag{4}$$

Heat transfer between the gas mixture and the ambient, $\dot{Q}_{\mathrm{amb}}$, occurred in the pipeline. It was determined by Equation (5) using the overall thermal conductance, UA, and a simple temperature difference evaluated at the inlet of the pipe segment. The ambient temperature was assumed to be 10 ° C.

$$\dot{Q}_{\mathrm{amb}} = UA\Delta T \quad \text{with} \quad \Delta T = T_{\mathrm{amb}} - T_{\mathrm{in}} \tag{5}$$

The thermal conductance was given from the total thermal resistance, R_{tot}, as in Equation (6). It was estimated by the thermal resistance of the soil and pipe wall, as the overall resistance from these two contributions were significantly greater than resistances from internal convection in the pipe. Two-dimensional heat transfer through the soil was assumed and modeled using a shape factor, S_f, and a thermal conductivity of soil, λ, of 2.4 W(m K)$^{-1}$ [9] while a thermal conductivity of 15.9 W(m K)$^{-1}$ [20] was assumed for the steel pipes.

$$UA = \frac{1}{R_{\mathrm{tot}}} \quad \text{with} \quad R_{\mathrm{tot}} \approx R_{\mathrm{soil}} + R_{\mathrm{wall}} = \frac{1}{S_f \lambda_{\mathrm{soil}}} + \frac{\ln\left(\frac{D_{\mathrm{o}}}{D_{\mathrm{i}}}\right)}{2\pi\lambda_{\mathrm{steel}}} \tag{6}$$

The shape factor was determined using a corrected burial depth, d_{cor}, which takes into account the thermal resistance at the soil surface by a second term where R_{cor} is 0.0685 m^{2}K W^{-1} [22].

$$S_f = \frac{2\pi L}{\ln\left(4d_{\mathrm{cor}}/D_{\mathrm{o}}\right)} \quad \text{with} \quad d_{\mathrm{cor}} = d + R_{\mathrm{cor}}\lambda_{\mathrm{soil}} \tag{7}$$

Finally, an energy balance was applied according to Equation (8).

$$\dot{Q}_{\mathrm{amb}} = \dot{m}\Delta h \tag{8}$$

2.5. Economic model

The economic analysis comprised the capital expenses and the operational expenses estimated for the whole lifetime of the compression system and pipeline. The capital expenses for the compression process were determined based on the size of each component, j, and the cost of a reference size of the same type of component summarised in Table 3. The purchased equipment cost (PEC) was calculated using the economies-of-scale relation given in Equation (9), where α is the scaling exponent from Table 3.

Table 3. Size and cost of reference components for capital expense estimation of compression process. All costs are given in CEPCI1000 [15].

Component type	**Reference size, X_{ref}**	**Reference cost, $\mathrm{PEC}_{\mathrm{ref}}$**	**Scaling exponent, α**
Reciprocating compressor	100 kW	180 000 USD	0.79
Screw compressor	300 kW	475 000 USD	0.77
Plate heat exchanger	100 m^2	51 600 USD	0.65
Pressure vessel	20 m$^{5/2}$	100 000 USD	0.81

$$\mathrm{PEC}_j = \mathrm{PEC}_{\mathrm{ref}} \left(\frac{X_j}{X_{\mathrm{ref}}}\right)^{\alpha} \tag{9}$$

To determine the total capital expenses (CAPEX) associated with the compression process, the Enhanced Detailed Factor Method described by Aromada *et al.* [23] was applied. The reference costs given in Table 2 are given in USD-CEPCI1000 for carbon steel components. The costs were converted to EUR2023 and machined stainless steel using a material factor of 1.3 [23], an average exchange rate of 1.08 USD EUR^{-1}, and the Chemical Engineering Plant Cost Index (CEPCI). The total capital expenses associated with the compression process were then given by Equation (10).

$$\mathrm{CAPEX}_{\mathrm{comp}} = \sum_j \mathrm{CAPEX}_j \tag{10}$$

The capital expenses of the pipeline were comprised of four elements given in Equation (11), as suggested by Skaugen *et al.* [9]. The labor cost, right-of-way (ROW), and miscellaneous costs were based on correlations for natural gas pipelines developed by Brown *et al.* [24]. However, Knoope *et al.* [25] emphasize the need for estimating the material costs for CO_2 pipelines based on the weight of the pipeline, as the amount of material and thereby costs might differ significantly to that of natural gas pipelines.

$$\mathrm{CAPEX}_{\mathrm{pipe}} = \mathrm{CAPEX}_{\mathrm{material}} + \mathrm{CAPEX}_{\mathrm{labor}} + \mathrm{CAPEX}_{\mathrm{ROW}} + \mathrm{CAPEX}_{\mathrm{misc}} \tag{11}$$

An economies-of-scale relation was fitted to a set of prices retrieved from a CO_2 pipeline supplier for various diameters and lengths to determine a correlation for the material cost of carbon steel pipelines. The relation in Equation (12) showed a

coefficient of determination of $R^2 = 0.797$ and is based on the specific mass per meter of the pipeline, m_{spec}. The prices were converted to welded stainless steel pipelines using a material factor of 1.75 [23]. A density of 8000 kg m^{-3} of stainless steel was used [20]. The costs from Equation (12) were converted from EUR2024 to EUR2023 using CEPCI.

$$\mathrm{CAPEX}_{\mathrm{material}} = L\left(11.498(m_{\mathrm{spec}})^{0.5351}\right) \quad \text{with} \quad m_{\mathrm{spec}} = \frac{\pi}{4}\rho\left(D_{\mathrm{o}}^2 - (D_{\mathrm{o}} - 2t)^2\right) \tag{12}$$

The costs of manpower, ROW, and miscellaneous were estimated using cost relations for natural gas pipelines in the "Mid-Atlantic" region of the US developed by Brown *et al.* [24] as it was estimated that the topography and economic status of Denmark resembles this region. The relations are given in Equation (13) where the diameter and pipe length are in inches and miles, respectively. The costs in Equation (13) are given in USD2018 and were converted to EUR2023 using the average exchange rate and the Employment Cost Index for the labor costs and the Producer Price Index for the refined petroleum product pipeline transport industry for ROW and miscellaneous costs.

$$\mathrm{CAPEX}_{\mathrm{labor}} = DL\left(43692\frac{D^{0.05683}}{L^{0.10108}}\right),\ \mathrm{CAPEX}_{\mathrm{ROW}} = DL\left(1942\frac{D^{0.17394}}{L^{0.01555}}\right),\ \mathrm{CAPEX}_{\mathrm{misc}} = DL\left(14616\frac{D^{0.16354}}{L^{0.16186}}\right) \tag{13}$$

The total capital expenses were annualized and discounted assuming a lifetime (Y) of 25 years [26] and a discount rate (r) of 3.5 % [27] as given in Equation (14). Operational expenses were assumed to be constant throughout the lifetime of the system and included fixed operation and maintenance and the costs of electricity and process cooling. The fixed operation and maintenance of rotary equipment was assumed to be 5 % of capital expenses every year while it was 3 % for all remaining equipment (including the pipeline) [26]. The cost of electricity was assumed to be 93.8 EUR2023 MWh^{-1} [28] and the cost of cooling water was set to 0.0962 EUR2023 m^{-3} [26].

$$\mathrm{CAPEX}_{\mathrm{annual}} = (\mathrm{CAPEX}_{\mathrm{comp}} + \mathrm{CAPEX}_{\mathrm{pipe}})\left(\frac{r(1+r)^Y}{(1+r)^Y - 1}\right) \tag{14}$$

A levelized cost (LC) per unit of transported gas was defined as given in Equation (15). It takes the overall system costs and divides it on a mass basis to the delivered CO_2 mixture, i.e. the mass flow rate of the gas entering the pipeline. The plant was assumed to operate 8000 hours annually.

$$\mathrm{LC} = \frac{\mathrm{CAPEX}_{\mathrm{annual}} + \mathrm{OPEX}_{\mathrm{fix}} + \mathrm{OPEX}_{\mathrm{el}} + \mathrm{OPEX}_{\mathrm{cool}}}{\dot{m} \cdot 8000\,\mathrm{h} \cdot 3600\,\mathrm{s\,h^{-1}}} \tag{15}$$

2.6. Sensitivity analysis

A sensitivity analysis was performed to investigate some of the variables expected to have the greatest influence on the economic relation between the compression process and pipeline transport. These included the isentropic efficiency of the compressors, the electricity price, and the capital expenses of the pipeline. Upper and lower estimates were identified for each variable. The isentropic efficiencies were decreased and increased with 5 %pt. for both reciprocating and screw compressors. For the electricity price, the upper and lower variables were given as the 90-percentile electricity prices of the Danish spot market price in 2023 including tariffs, and were set to 33 EUR MWh^{-1} and 163 EUR MWh^{-1}. For the capital expenses of the pipeline, two alternative sets of cost relations developed by Brown *et al.* [24] were used. The "Great Plains and Rocky Mountains" and "New England" regions were used for the lower and upper estimates, respectively, as these in general showed lower and higher costs compared to the "Mid-Atlantic" region in the study by Brown *et al.* [24].

3. Results

3.1. Optimal pipe diameters

Simulations were performed where the nominal diameter (DN) for each combination of mass flow rate and distance was varied to determine the economic optimal pipe size. The results are shown for the delivery pressure of 2 bar in Fig 2 where each subplot represents a mass flow rate of CO_2 and the markers represent different transport distances. The diameter yielding the lowest levelized costs for each distance is marked by a black border. Choosing the optimal diameter was more important for longer transport distances (20 km to 35 km), especially when the gas flow rate was low (0.5 t h^{-1} to 1 t h^{-1}). With shorter transport distances (1 km to 5 km), the cost difference between different pipe sizes was less significant. With longer transport distances, the capital investment of the pipeline would increase and thereby make it relatively more important for the overall costs. The costs were therefore more dependant on the pipe size for longer distances.

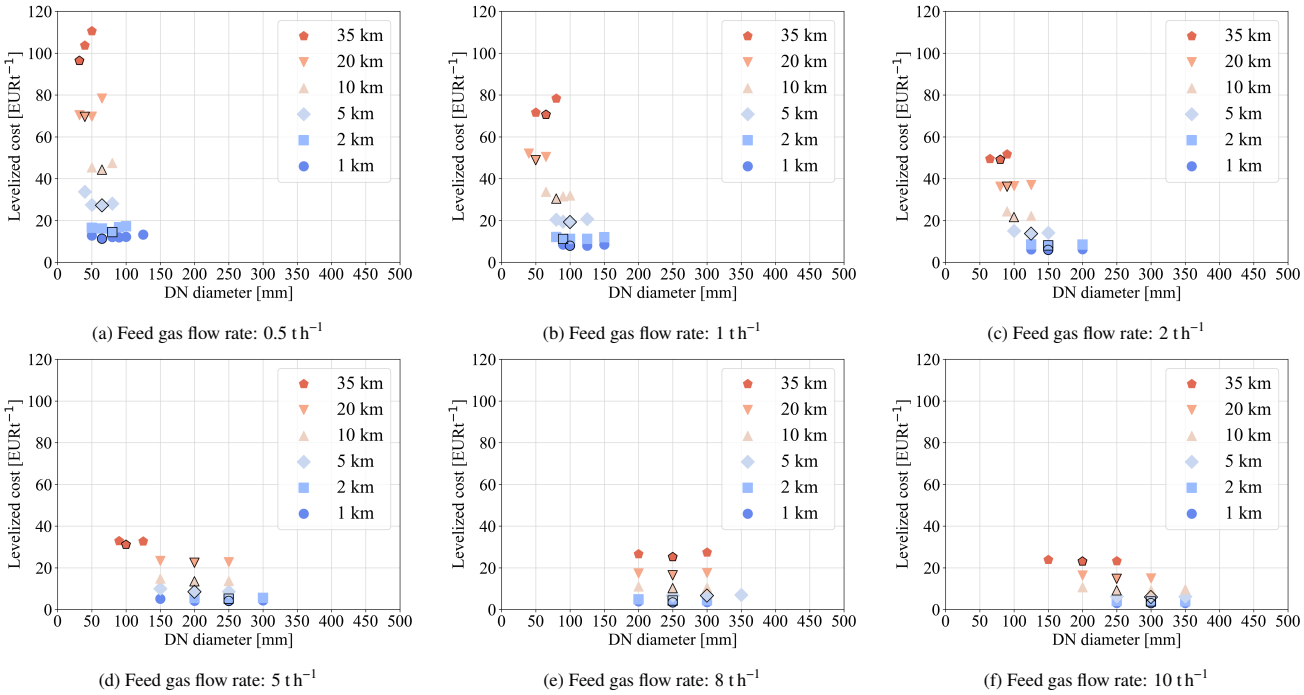

(a) Feed gas flow rate: 0.5 t h^{-1} (b) Feed gas flow rate: 1 t h^{-1} (c) Feed gas flow rate: 2 t h^{-1}

(d) Feed gas flow rate: 5 t h^{-1} (e) Feed gas flow rate: 8 t h^{-1} (f) Feed gas flow rate: 10 t h^{-1}

Fig 2. Levelized cost of compression and pipeline transport when delivering the gas mixture at 2 bar for various pipe diameters at the investigated distances and mass flow rates. The diameters with lowest levelized costs are marked by a black border.

Fig 2 shows, that increasing the gas flow rate increased the optimal diameter. Furthermore, the diameter should generally be decreased when the transport distance increases, especially for mass flow rates up to 2 t h^{-1}. In these cases, the ratio between the costs of electricity consumption and the capital expenses of the pipeline showed to be important. There was an economic benefit from reducing the pipe diameter and thereby decreasing the capital expenses as well as increasing the pressure loss and pipeline inlet pressure which increased the electricity consumption of compression. This ratio was directly affected by the electricity price, the efficiency of the compressors, and the capital cost relations for the pipeline. These effects are further investigated in Section 3.3. The economic trade-off was less pronounced for larger mass flow rates. In these cases, the optimal diameter mostly depended on the mass flow rate, and was less dependant on the transport distance, especially for short distances (1 km to 5 km).

Similar simulations were performed for the delivery pressure of 18 bar, and the results are shown in Fig 3. Choosing the economic optimal diameter became slightly more important for the 18 bar option compared to the 2 bar option, especially for transport distances between 5 km to 35 km and smaller flow rates (0.5 t h^{-1} to 2 t h^{-1}). A different trend for the dependence between transport distance and optimal pipe size was also seen for the 18 bar option compared to the 2 bar option. Here, the pipe size should generally be the same size or increase as the transport distance became longer. This was most pronounced for the mass flow rates between 0.5 t h^{-1} to 5 t h^{-1}, while the pipe size was almost independent on the transport distance for large mass flow rates. The pressure level of the gas entering the pipeline was greater for delivery of 18 bar compared to 2 bar, resulting in a greater density. Therefore, the optimal diameters were smaller and the increase in pipe size had a relatively lower influence on the levelized costs. At the same time, more compressor power was needed to ensure the higher pressure of 18 bar at the pipe outlet. The increase in optimal diameter with increased transport distance indicates, that there was a greater economic benefit of reducing the pressure losses compared to the increased capital expenses of the pipeline.

3.2. Levelized costs for optimal diameters

With the optimal pipe diameter identified in Fig 2 and Fig 3, the levelized costs were split into the two parts associated with the compression process and pipeline transport as shown in Fig 4. A clear economies-of-scale relation was seen, both with the increase in transport distance and the mass flow rate for delivery pressures of both 2 bar and 18 bar. It was less expensive to deliver the gas mixture at 2 bar for all flow rates and transport distances. However, for long distances (20 km to 35 km) the cost difference between the two options was reduced, especially for smaller flow rates (0.5 t h^{-1} to 5 t h^{-1}).

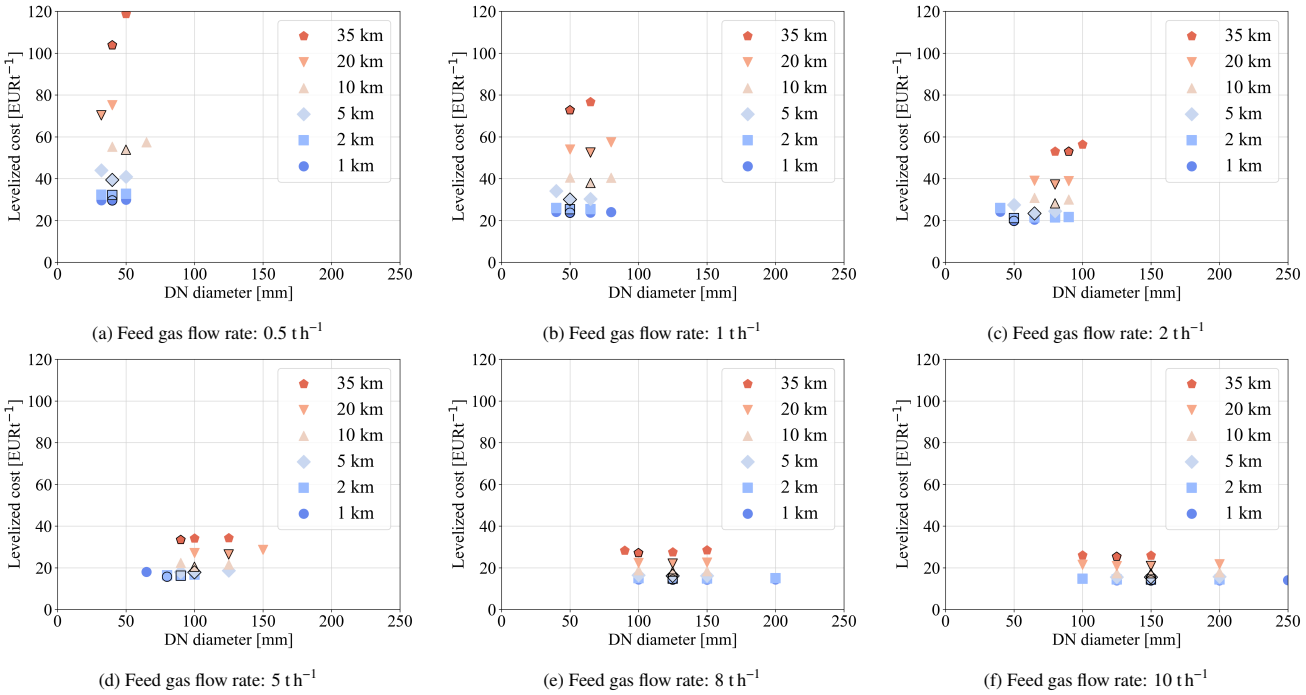

(a) Feed gas flow rate: 0.5 t h^{-1} (b) Feed gas flow rate: 1 t h^{-1} (c) Feed gas flow rate: 2 t h^{-1}

(d) Feed gas flow rate: 5 t h^{-1} (e) Feed gas flow rate: 8 t h^{-1} (f) Feed gas flow rate: 10 t h^{-1}

Fig 3. Levelized cost of compression and pipeline transport when delivering the gas mixture at 18 bar for various pipe diameters at the investigated distances and mass flow rates. The diameters with lowest levelized costs are marked by a black border.

The greater costs of delivering 18 bar were generally associated with higher compression costs. However, these costs were seen to be almost constant with different distances, meaning that the increase in costs for longer transport distances when delivering CO_2 at 18 bar was mostly affected by the greater capital expenses associated with a longer pipe. For delivery of the CO_2 at 2 bar, both the compression costs and pipeline capital expenses increased as the transport distance became longer. As identified in Fig 2, the pressure loss would increase due to smaller diameters which increased the compression power, and at the same time the pipeline became longer, increasing capital investment.

3.3. Sensitivity analysis

The results of the sensitivity analysis for delivering gas at 2 bar and 18 bar are shown in Fig 5 and Fig 6, respectively. Here the optimal diameters under the upper and lower estimates of the compressor efficiency, pipeline capital expenses, and the electricity price are seen. The enlarged ”X” is the base case while each of the other markers indicates the optimal diameter under a sensitivity case. The colors represent different transport distances. Generally, the same trends were identified for both pressure options and the three investigated parameter showed little to no effect on the choice of optimal pipe size. For example, a change in compressor efficiency would have little effect on the optimal pipe size, as the square and pentagon markers are mostly located on a vertical line with the ”X”. In some cases, the optimal diameter should be changed by one size.

The effect of the electricity price was slightly more significant. It mostly influenced the longer transport distances and large mass flow rates in a way, that a lower electricity price allowed for slightly smaller pipe sizes and thereby a larger pressure drop while a greater electricity price would increase the optimal pipe size in order to reduce the pressure drop. The upper estimate of the capital expenses showed greater influence. For small mass flow rates, the optimal diameter was generally of the same size or smaller, while it should always be smaller for larger mass flow rates. This could be attributed to the trade-off between compression costs and pipeline capital expenses. For larger mass flow rates the pipeline sizes were bigger, resulting in a relatively greater cost influence when increasing the estimate of the capital expenses. The lower estimate of the pipeline capital expenses showed a less significant influence, but did increase the optimal pipe size for some cases. The different sensitivity scenarios did not affect the trends for choosing optimal diameters when considering the increase in transport distances.

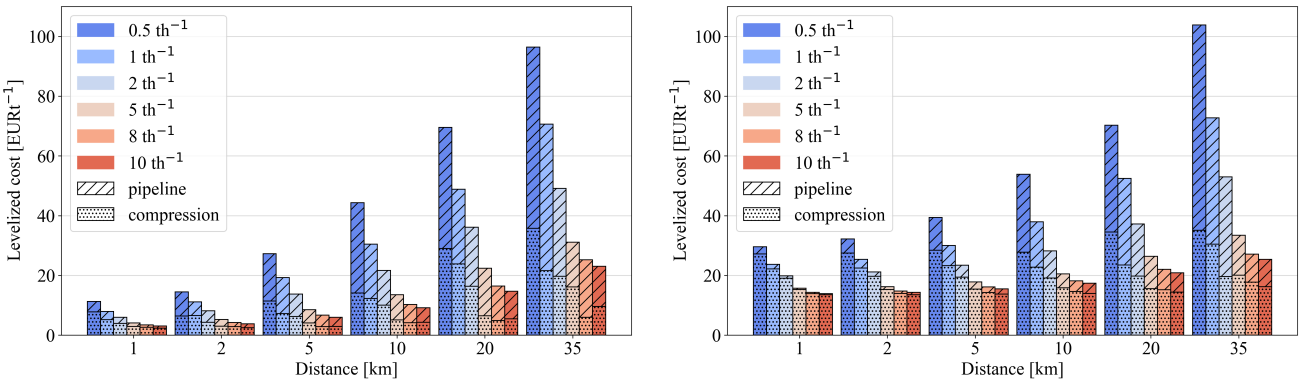

(a) Delivery at 2 bar.

(b) Delivery at 18 bar.

Fig 4. Levelized costs distributed between the compression process and pipeline for the investigated distances and mass flow rates.

The relative changes in levelized costs under the different sensitivity cases were determined. The minimum and maximum cost changes for delivery of gas at 2 bar and 18 bar are given in Table 4 and Table 5, respectively. The capital expenses was the most sensitive parameter followed by the electricity price while the compressor efficiency was less important. The capital expenses of the pipeline had a greater influence on the delivery of gas at 2 bar compared to 18 bar with the greatest relative cost changes of 530 % and 260 %, respectively. This can be attributed to the greater share of costs associated with the pipeline due to larger pipe sizes. Similarly, the cost of electricity was more important when delivering gas at 18 bar (up to 32 % change in cost), since the compression costs constituted a greater share of the total costs. Furthermore, the greatest cost effect due to changes in the electricity price was found for large mass flow rates and short distances. In these cases, the compression costs accounted for a greater share of the total costs, making the parameter more important.

Generally, the upper estimate for the capital expenses of the pipeline affected the levelized cost to the greatest extent, especially when the length of the pipeline was more than 10 km. The results indicate, that when optimizing the diameter for the given set of assumptions, the levelized cost was not greatly affected by uncertainties in the electricity price and compressor efficiency, especially for the case of delivering gas at 2 bar. However, higher capital investment of the pipeline

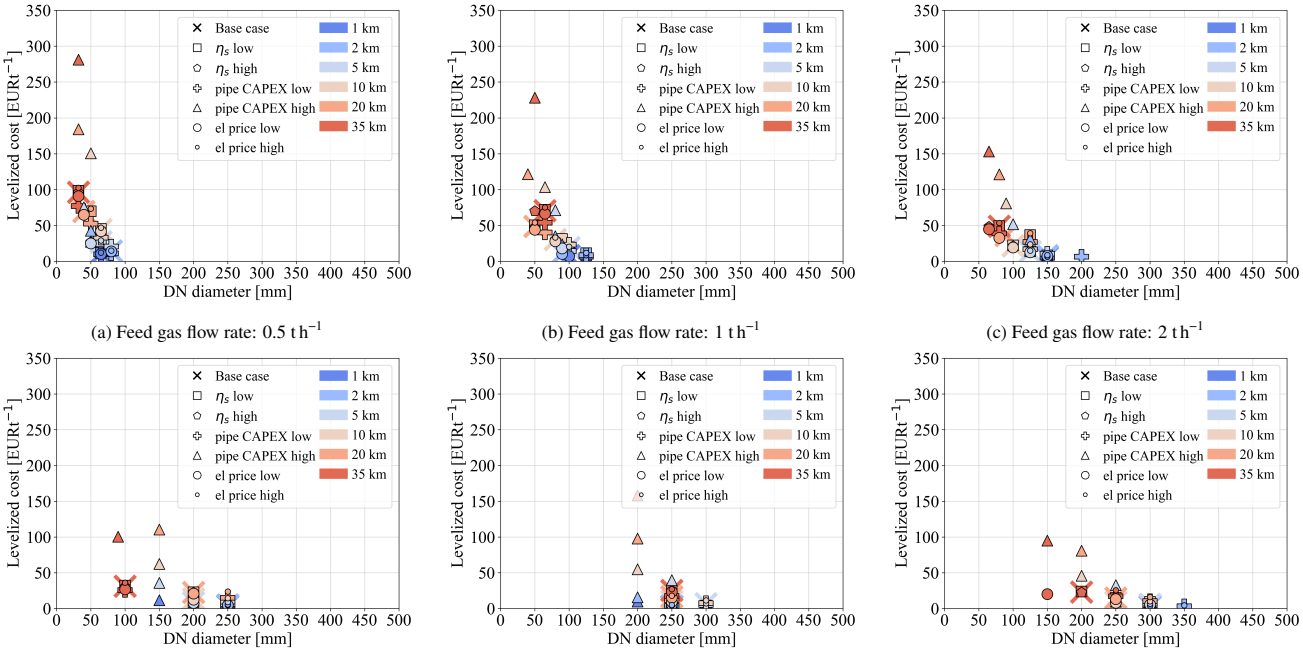

(a) Feed gas flow rate: 0.5 t h^{-1}

(b) Feed gas flow rate: 1 t h^{-1}

(c) Feed gas flow rate: 2 t h^{-1}

(d) Feed gas flow rate: 5 t h^{-1}

(e) Feed gas flow rate: 8 t h^{-1}

(f) Feed gas flow rate: 10 t h^{-1}

Fig 5. Sensitivity analysis of levelized cost of compression and pipeline transport when delivering the gas mixture at 2 bar.

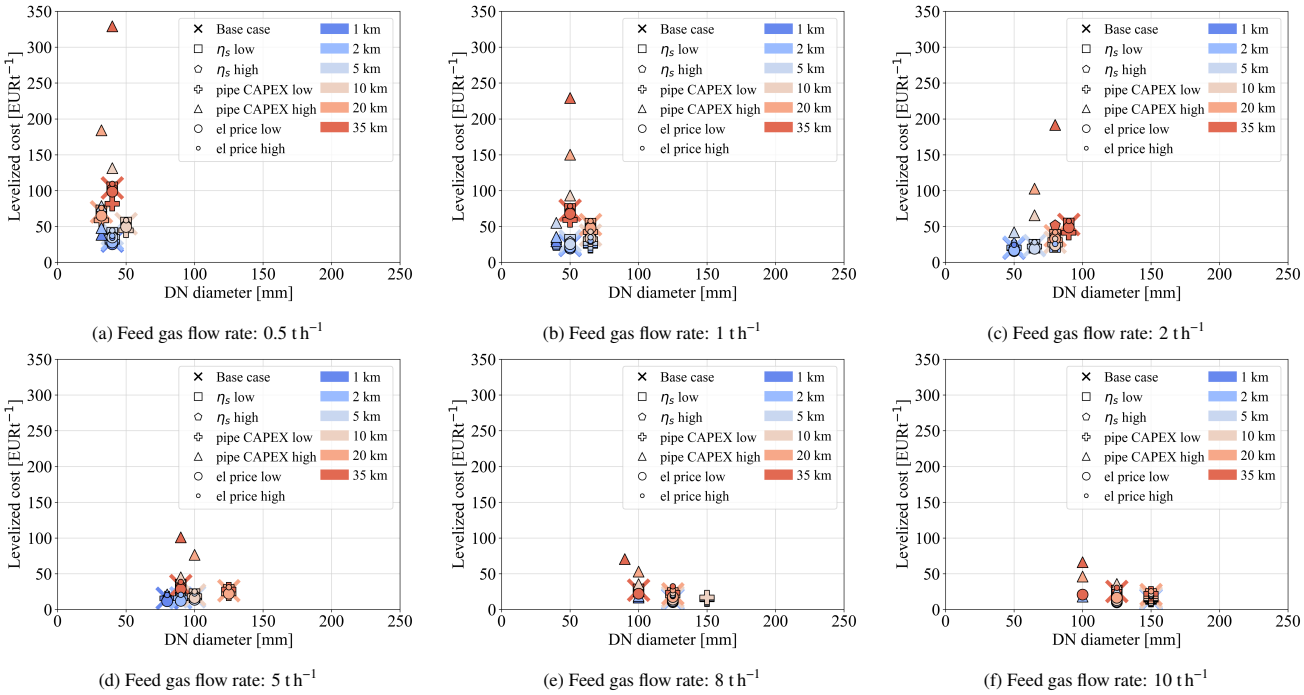

(a) Feed gas flow rate: 0.5 t h^{-1} (b) Feed gas flow rate: 1 t h^{-1} (c) Feed gas flow rate: 2 t h^{-1}

(d) Feed gas flow rate: 5 t h^{-1} (e) Feed gas flow rate: 8 t h^{-1} (f) Feed gas flow rate: 10 t h^{-1}

Fig 6. Sensitivity analysis of levelized cost of compression and pipeline transport when delivering the gas mixture at 18 bar.

can significantly affect the costs, especially for longer pipelines regardless of the delivery pressure.

Table 4. Minimum and maximum relative changes in the levelized costs for the sensitivity analysis when delivering gas at 2 bar.

		Compressor efficiency		Capital expenses of pipeline		Electricity price	
	Unit	lower	upper	lower	upper	lower	upper
minimum change	%	0.061	–3.4	–33	140	–15	3.7
maximum change	%	3.9	2.0	–11	530	– 3.2	17

Table 5. Minimum and maximum relative changes in the levelized costs for the sensitivity analysis when delivering gas at 18 bar.

		Compressor efficiency		Capital expenses of pipeline		Electricity price	
	Unit	lower	upper	lower	upper	lower	upper
minimum change	%	0.77	–5.1	–22	16	–28	5.5
maximum change	%	5.8	3.9	– 1.2	260	– 4.8	32

4. Discussion

Both positive and negative cost changes were seen for changes in the compressor efficiency in the sensitivity analysis. The number of compressors was chosen to ensure the pressure ratio over each compressor did not exceed four. This means, that the cost change for different diameters could be discontinuous when different inlet pressures were needed. This also applied to the estimate of the capital expenses of the compression equipment. The EDF method [23] uses a piping factor based on the purchased equipment cost. The piping factor is increased in discrete steps for increasing intervals of purchased equipment costs. This results in a discontinuity. For some cases in the sensitivity analysis, the compressor size would increase just enough for the purchased equipment cost to be within a new cost interval resulting in a decreased piping factor in the EDF method. This could lead to an overall decrease in the total capital investment of the compressor. Therefore, both positive and negative cost changes were seen for the upper estimate of the compressor efficiency.

Not all existing pipe sizes were investigated. Through trial and error, the relevant range of diameters that yielded the minimum levelized cost was found. Nearby sizes were included in the simulations to ensure a minimum was found. However, the smallest pipe size included in the analysis was typically limited by a significantly larger pressure loss, which

resulted in great variations in density and velocity along the pipeline. Furthermore, there was a cut-off for excluding pipe sizes where the inlet pressure became so high, that a large share of the gas condensed during the transport process as the gas was cooled down in the beginning of the pipeline. The maximum allowed pressure in the simulations was 52 bar. For reference, the boiling point pressure at the ambient temperature is 57 bar for the inlet composition. Similarly, the greatest pipe size included in the analysis was limited by a requirement for a slight overpressure. The change in optimal diameters for the sensitivity analysis might be restricted by these cut-off criteria.

It should be further investigated how acceptable minimum and maximum velocities of a gaseous flow through a pipeline can be determined. According to Peletiri *et al.* [29] the API RP 14E erosional velocity equation can be used to determine the maximum allowed velocity, however, this is not recommended by Sani *et al.* [30] as the equation is too generic. Using the equation, a maximum velocity at the outlet of the pipe for the 2 bar and 18 bar delivery yields around 63 $m\,s^{-1}$ and 20 $m\,s^{-1}$, respectively. All the optimal pipe sizes showed velocities lower than these limits. Knoope *et al.* [5] set the limit of gaseous transport between 5 $m\,s^{-1}$ to 20 $m\,s^{-1}$. For some of the 18 bar cases, the velocities were lower than this limit, indicating that smaller pipe sizes should be used. Similarly, some cases with delivery of 2 bar and long transport distances had both inlet and outlet velocities outside this range. In such case, larger pipe diameters should be used to reduce the change in fluid density along the pipeline. Alternatively, it could be relevant to optimize the size of multiple pipe segments allowing the diameter to be adjusted along the pipeline.

During intercooling in the compression process, water was condensed and removed. The amount of water that can be removed in this process, depends on the composition of the CO_2 mixture, the pressure level, and available cooling temperature. In all cases, the gas mixture was saturated with water at the inlet of the pipeline and the amount of water decreased with greater inlet pressures. For delivery of gas at 18 bar, the presence of water was therefore generally lower, ranging between 3000 ppm to 4600 ppm (molar). For delivery of gas at 2 bar it was between 2900 ppm to 32300 ppm (molar). This is significantly greater than the recommended water content in transport of purified CO_2 [8]. As the gas travels through the pipeline, heat will be lost to the surroundings resulting in a temperature decrease. Depending on the pressure loss, this can result in the formation of free water within the pipeline, which is known to increase the corrosion rate. Some measures to avoid this could be insulation of the pipeline or using liquid separation techniques along the pipeline. The distance travelled before the gas reaches the temperature of the ambient increases as the gas flow rate increases. Furthermore, it is greater for smaller pipe sizes as the heat transfer area decreases. Future studies should take this aspect into account when choosing the optimal diameter for different gas flow rates and distances as there might be technical limitations or economic penalties for some pipe sizes to reduce the presence of free water.

5. Conclusion

A technoeconomic analysis of a system comprising compression and pipeline transport of unconditioned gaseous CO_2 from a small biogas facility to a central conditioning system was made. The gas was delivered either at 2 bar or 18 bar, corresponding to the central conditioning unit entailing both compression, purification, and liquefaction or only purification and liquefaction. The gas flow rates were varied according to relevant sizes of Danish biogas facilities between 0.5 $t\,h^{-1}$ to 10 $t\,h^{-1}$ and the transport distances were varied from 1 km to 35 km. The pipeline size was optimized for each case from an economic perspective. The study showed that it was more important to optimize the pipeline diameter for transport distances of 10 km or longer and for mass flow rates of 2 $t\,h^{-1}$ or less. In these cases, the optimal pipe diameter was decreased as the transport distance became longer for the delivery of gas at 2 bar, while the optimal pipe diameters were either slightly increased or unaffected by an increased transport distance at the delivery of gas at 18 bar. Generally, larger pipe sizes were needed for the delivery of gas at 2 bar compared to 18 bar ranging between DN32 to DN300 and DN32 to DN150, respectively.

It was cheaper to deliver the CO_2 at 2 bar compared to 18 bar for flow rates of more than 2 $t\,h^{-1}$ and transport distances of 20 km or less as the costs ranged between 3.0 EUR t^{-1} to 44 EUR t^{-1} and 14 EUR t^{-1} to 54 EUR t^{-1}, respectively. The cost difference became insignificant for flow rates of 2 $t\,h^{-1}$ or less and transport distances of 20 km to 35 km, ranging between 36 EUR t^{-1} to 96 EUR t^{-1} and 37 EUR t^{-1} to 104 EUR t^{-1} for the delivery pressure of 2 bar and 18 bar, respectively. The generally higher costs associated with the delivery of gas at 18 bar was due to higher compression costs which constituted between 34 % to 97 % of the total costs. Therefore, the 18 bar option showed a greater sensitivity to the electricity price.The capital expenses of the pipeline showed the greatest importance for both delivery pressures. The results of this study should be used in future analyses comprising also the purification and liquefaction system to identify under which mass flow rates

and distances it is more economically beneficial to perform central conditioning as opposed to local conditioning at the bio-methane production facilities.

References

[1] Danish Energy Agency, "Point sources of CO_2 - potentials for CCS and CCUS," Tech. Rep., 2023, [in Danish]. [Online]. Available: ens.dk/sites/ens.dk/files/CCS/punktkilder_til_co2_-_potentialer_for_ccs_og_ccu_2022-opdatering.pdf.

[2] Danish Energy Agency, "Technology data for renewable fuels," Tech. Rep., 2024. [Online]. Available: ens.dk/sites/ens.dk/files/Analyser/technology_data_for_renewable_fuels.pdf.

[3] C. Kolster, E. Mechleri, S. Krevor, and N. M. Dowell, "The role of CO_2 purification and transport networks in carbon capture and storage cost reduction," *International Journal of Greenhouse Gas Control*, vol. 58, pp. 127–141, Mar. 2017, ISSN: 17505836. DOI: 10.1016/j.ijggc.2017.01.014.

[4] S. Roussanaly, N. Berghout, T. Fout, *et al.*, "Towards improved cost evaluation of carbon capture and storage from industry," *International Journal of Greenhouse Gas Control*, vol. 106, Mar. 2021, ISSN: 17505836. DOI: 10.1016/j.ijggc.2021.103263.

[5] M. M. Knoope, A. Ramírez, and A. P. Faaij, "Economic optimization of CO_2 pipeline configurations," *Energy Procedia*, vol. 37, pp. 3105–3112, 2013, ISSN: 18766102. DOI: 10.1016/j.egypro.2013.06.196.

[6] H. Lu, X. Ma, K. Huang, L. Fu, and M. Azimi, "Carbon dioxide transport via pipelines: A systematic review," *Journal of Cleaner Production*, vol. 266, Sep. 2020, ISSN: 09596526. DOI: 10.1016/j.jclepro.2020.121994.

[7] M. Vitali, F. Corvaro, B. Marchetti, and A. Terenzi, "Thermodynamic challenges for CO_2 pipelines design: A critical review on the effects of impurities, water content, and low temperature," *International Journal of Greenhouse Gas Control*, vol. 114, Feb. 2022, ISSN: 17505836. DOI: 10.1016/j.ijggc.2022.103605.

[8] V. E. Onyebuchi, A. Kolios, D. P. Hanak, C. Biliyok, and V. Manovic, "A systematic review of key challenges of CO_2 transport via pipelines," *Renewable and Sustainable Energy Reviews*, vol. 81, pp. 2563–2583, Jan. 2018, ISSN: 18790690. DOI: 10.1016/j.rser.2017.06.064.

[9] G. Skaugen, S. Roussanaly, J. Jakobsen, and A. Brunsvold, "Techno-economic evaluation of the effects of impurities on conditioning and transport of CO_2 by pipeline," *International Journal of Greenhouse Gas Control*, vol. 54, pp. 627–639, Nov. 2016, ISSN: 17505836. DOI: 10.1016/j.ijggc.2016.07.025.

[10] D. Y. Peng and D. B. Robinson, "A new two-constant equation of state," *Industrial and Engineering Chemistry Fundamentals*, vol. 15, pp. 59–64, 1 1976, ISSN: 01964313. DOI: 10.1021/i160057a011.

[11] J. N. Jaubert and F. Mutelet, "Vle predictions with the Peng-Robinson equation of state and temperature dependent k_{ij} calculated through a group contribution method," *Fluid Phase Equilibria*, vol. 224, pp. 285–304, 2 Oct. 2004, ISSN: 03783812. DOI: 10.1016/j.fluid.2004.06.059.

[12] X. Xu, S. Lasala, R. Privat, and J. N. Jaubert, "E-PPR78: A proper cubic eos for modelling fluids involved in the design and operation of carbon dioxide capture and storage (CCS) processes," *International Journal of Greenhouse Gas Control*, vol. 56, pp. 126–154, Jan. 2017, ISSN: 17505836. DOI: 10.1016/j.ijggc.2016.11.015.

[13] A. Chapoy, M. Nazeri, M. Kapateh, R. Burgass, C. Coquelet, and B. Tohidi, "Effect of impurities on thermophysical properties and phase behaviour of a CO_2-rich system in ccs," *International Journal of Greenhouse Gas Control*, vol. 19, pp. 92–100, 2013, ISSN: 17505836. DOI: 10.1016/j.ijggc.2013.08.019.

[14] S. Klein, *EES: Engineering equation solver*. [Online]. Available: https://fchartsoftware.com/ees/.

[15] D. R. Woods, *Rules of Thumb in Engineering Practice*. Wiley-VCH Verlag GmbH & Co., 2007, ISBN: 9783527312207.

[16] M. Souders and G. G. Brown, "Design of fractionating columns i. entrainment and capacity," *Industrial and Engineering Chemistry*, vol. 26, pp. 98–103, 1 Jan. 1934. DOI: 10.1021/ie50289a025. [Online]. Available: https://pubs.acs.org/sharingguidelines.

[17] R. Turton, R. C. Bailie, W. B. Whiting, and J. A. Shaewitz, *Analysis, Synthesis, and Design of Chemical Processes*, 3rd ed. Pearson Education, Inc., 2009, ISBN: 9780135129661.

[18] ASME, *Welded and seamless wrought steel pipe b36.10*, 2018.

[19] Council directive 2014/68/EU, *On the harmonisation of the laws of the member states relating to the making available on the market of pressure equipment*, 2014. [Online]. Available: https://data.europa.eu/eli/dir/2014/68.

[20] W. D. Callister and D. G. Rethwisch, *Materials Science and Engineering*, 9th ed. John Wiley Sons, 2015, ISBN: 978-1-118-31922-2.

[21] F. M. White, *Fluid Mechanics*, 8th. McGraw-Hill Education, 2016, ISBN: 9789814720175.

[22] B Kvisgaard and S Hadvig, "Heat loss from pipelines in district heating systems," Technical University of Denmark, Tech. Rep., 1980.

[23] S. A. Aromada, N. H. Eldrup, and L. E. Øi, "Capital cost estimation of CO_2 capture plant using enhanced detailed factor (edf) method: Installation factors and plant construction characteristic factors," *International Journal of Greenhouse Gas Control*, vol. 110, Sep. 2021, ISSN: 17505836. DOI: 10.1016/j.ijggc.2021.103394.

[24] D. Brown, K. Reddi, and A. Elgowainy, "The development of natural gas and hydrogen pipeline capital cost estimating equations," *International Journal of Hydrogen Energy*, vol. 47, pp. 33 813–33 826, 79 Sep. 2022, ISSN: 03603199. DOI: 10.1016/j.ijhydene.2022.07.270.

[25] M. M. Knoope, A. Ramírez, and A. P. Faaij, "A state-of-the-art review of techno-economic models predicting the costs of CO_2 pipeline transport," *International Journal of Greenhouse Gas Control*, vol. 16, pp. 241–270, 2013, ISSN: 17505836. DOI: 10.1016/j.ijggc.2013.01.005.

[26] E. H. Jensen, R. C. Pedersen, I. A. Løge, *et al.*, "The cost of impurities: A tehcno-economic assessment on conditioning of captured CO_2 to commercial specifications," *International Journal of Greenhouse Gas Control*, 2024. DOI: 10.2139/ssrn.4774399.

[27] D. M. of Finance, "Guideline for socioeconomic impact assessment," Tech. Rep., Jun. 2024, [in Danish]. [Online]. Available: https://fm.dk/arbejdsomraader/regnemetoder-og-regnemodeller/vejledning-om-samfundsoekonomiske-konsekvensvurderinger/.

[28] R. C. Pedersen, E. Rothuizen, T. Ommen, and J. K. Jensen, "Technoeconomic optimisation of systems for liquefaction and purification of captured CO_2," in *26th International Congress of Refrigeration*, 2023, pp. 358–369. DOI: 10.18462/iir.icr.2023.0707.

[29] S. P. Peletiri, N. Rahmanian, and I. M. Mujtaba, "CO_2 pipeline design: A review," *Energies*, vol. 11, 9 Sep. 2018, ISSN: 19961073. DOI: 10.3390/en11092184.

[30] F. M. Sani, S. Huizinga, K. A. Esaklul, and S. Nesic, "Review of the api rp 14e erosional velocity equation: Origin, applications, misuses, limitations and alternatives," *Wear*, vol. 426-427, pp. 620–636, Apr. 2019, ISSN: 00431648. DOI: 10.1016/j.wear.2019.01.119.